ANALYSIS OF STABILITY AND ENVIRONMENTAL DECONTAMINATION STRATEGY FOR A FRACTIONAL-ORDER EBOLA MODEL FOR BAT POPULATION

ZINEB EL RHOUBARI[1,*], MOUSSA BACHRAOUI[2], KHALID HATTAF[2,3]

[1]Laboratory of Fundamental Mathematics and their Applications, Chouaib Doukkali University, EL Jadida 24000, Morocco

[2]Laboratory of Analysis, Modeling and Simulation, Faculty of Sciences Ben MSick, Hassan II University of Casablanca, Sidi Othman, Casablanca P.O. Box 7955, Morocco

[3]Equipe de Recherche en Modélisation et Enseignement des Mathématiques (ERMEM), Centre Régional des Métiers de l'Education et de la Formation (CRMEF), Derb Ghalef, Casablanca 20340, Morocco

Abstract. Bats are known reservoirs of the Ebola virus, making the control of the disease within bat population crucial for preventing human outbreaks. This study presents a fractional-order Ebola model to describe the dynamics of Ebola virus disease (EVD) in bat population, incorporating memory effects to provide a more accurate representation of disease spread compared to traditional integer-order models. We analyze the model's global properties, including stability and equilibrium points, and propose a time-dependent environmental decontamination control strategy aimed at minimizing the number of infectious bats while reducing associated costs. Using numerical simulations with specialized methods for fractional-order systems, we validate the theoretical results and demonstrate the effectiveness of the control strategy. The findings highlight that the proposed control significantly reduces the number of infectious bats, underscoring environmental decontamination as a viable measure for EVD control in bat population.

Keywords: Ebola; bats; fractional; control; stability.

2020 AMS Subject Classification: 92D30, 26A33, 37N25.

---

*Corresponding author

E-mail address: zineb.elrhoubari@gmail.com

1. INTRODUCTION

EVD is one of the most severe and life-threatening infectious diseases known to humanity. It is caused by the Ebola virus, a member of the Filoviridae family, and was first identified in 1976 during simultaneous outbreaks in what is now the Democratic Republic of Congo (DRC) and South Sudan. Since its discovery, the disease has become a recurring health crisis, particularly in regions of sub-Saharan Africa, where healthcare systems face significant challenges in containing its spread. The virus is notorious for its ability to cause sudden, severe outbreaks with high mortality rates and devastating social and economic consequences.

Over the years, the statistics associated with Ebola have painted a grim picture of its impact. The largest recorded outbreak occurred between 2014 and 2016 in West Africa, where the disease claimed more than 11,000 lives out of over 28,600 reported cases, highlighting a mortality rate of nearly 40% [1]. Smaller outbreaks, while less catastrophic, also underscore the danger posed by this virus, which can have fatality rates ranging from 25% to 90% depending on access to medical care and the timing of intervention. The second-largest outbreak was recently declared in the DRC in August 2018, claiming approximately 2299 lives by July 2020 [2].

EVD has a significant ecological connection with bats, which are widely believed to be the natural reservoir of the virus. While the exact origins of Ebola remain under investigation, mounting evidence suggests that fruit bats of the Pteropodidae family play a critical role in the virus's life cycle [3]. These bats can carry the virus without exhibiting symptoms, allowing it to persist in nature and potentially spill over into other species, including humans.

The transmission of the Ebola virus from bats to humans often occurs indirectly. Bats may infect other wildlife, such as primates or duikers, when they shed the virus through saliva, feces, or urine [4, 5]. Humans can then contract the virus through contact with these infected animals, typically via hunting, handling, or consumption of bushmeat [6, 7]. In some cases, direct human exposure to bat secretions or bites has also been linked to initial cases of outbreaks. For instance, during the 2007 outbreak in Luebo in DRC, epidemiological investigations revealed that the first human victim had purchased freshly killed bats from hunters for consumption [8]. This activity was linked to the subsequent human-to-human transmission events that led to the outbreak. Similarly, in the 2014–2016 West African Ebola epidemic, the index case was traced

to a two-year-old child in Meliandou in Guinea [9]. Researchers believe the child contracted the virus through direct contact with insectivorous bats from a colony near the village. This initial zoonotic transmission was followed by human-to-human spread, resulting in a widespread epidemic.

The role of bats in Ebola ecology is particularly significant because of their widespread habitat and interaction with human communities. In regions where bats are hunted for food or their habitats overlap with agricultural and settlement areas, the risk of zoonotic spillover increases. Certain cultural practices, such as the preparation and consumption of bat meat, can amplify the likelihood of human exposure to the virus.

Mathematical modeling has become an essential tool in understanding the spread of EVD within bat population and its transmission to other species. Early models focused on mapping the spatial distribution of infected bats, providing critical insights into high-risk areas. For instance, the study [10] used statistical and computational models to predict regions where bats infected with filoviruses, including Ebola, are likely to be found. This approach has proven valuable for disease monitoring and control efforts. Another study modeled bat-to-bat transmission using bilinear incidence functions, assuming that infected bats do not recover from the virus [11].

Building on these efforts, Rhoubari et al. [12] enhanced the epizootic model from [11] by introducing a cure rate and developing two generalized incidence functions. These functions account for various transmission dynamics described in the literature, such as bilinear incidence, saturated incidence, the Beddington-DeAngelis functional response, the Crowley-Martin functional response, and the Hattaf-Yousfi functional response. A specific case of this model was later analyzed in [13], focusing on the impact of memory and saturated incidence functions. Moreover, in [14], the authors proposed and analyzed a reaction-diffusion model using partial differential equations to explore the spatial dynamics of Ebola virus diffusion within bat population.

Research into the unique immune system of bats has shed light on their ability to coexist with pathogens like EVD [15, 16, 17]. Bats have evolved immune responses that enable them to tolerate infections that are lethal to other species. Studies have highlighted how these immune

adaptations allow bats to serve as reservoirs for numerous viruses without experiencing severe symptoms. Understanding these mechanisms is crucial for developing strategies to mitigate the spread of EVD and other zoonotic diseases. Considering these ecological and mathematical perspectives, we propose to advance the understanding of EVD dynamics within bat population by studying a fractional-order model. Unlike traditional integer-order models, fractional-order models offer greater flexibility in capturing the memory and hereditary properties of biological systems, which are critical in the context of EVD transmission. This approach allows for a more nuanced representation of the complex interactions between bats, the virus, and the environment. In addition, we will incorporate an optimal control strategy focusing on environmental decontamination. This strategy aims to reduce the contamination of bats, the initial source of Ebola, from contamined environment and minimize the risk of virus transmission from bats to other species and ultimately to humans.

The proposed fractional-order model for Ebola transmission in bat population considers direct transmission through contact with infectious bats and indirect transmission via a contaminated environment, where infectious bats shed the virus. This fractional-order model, in the absence of control measures, is described by:

$$(1) \quad \begin{cases} {}^{C}_{0}\mathscr{D}^{\alpha}_{t} P_1(t) = \beta^{\alpha} - m^{\alpha} P_1 - \lambda_1^{\alpha} P_1 P_2 - \lambda_2^{\alpha} P_1 Q, \\ {}^{C}_{0}\mathscr{D}^{\alpha}_{t} P_2(t) = \lambda_1^{\alpha} P_1 P_2 + \lambda_2^{\alpha} P_1 Q - (m^{\alpha} + r^{\alpha}) P_2, \\ {}^{C}_{0}\mathscr{D}^{\alpha}_{t} P_3(t) = r^{\alpha} P_2 - m^{\alpha} P_3, \\ {}^{C}_{0}\mathscr{D}^{\alpha}_{t} Q(t) = \delta^{\alpha} P_2 - e^{\alpha} Q. \end{cases}$$

The variables and parameters of system (1) are defined in the following table.

As described in [18], we adopt a fractional-order system in which all terms are raised to the fractional power α. This approach ensures the unified application of fractional-order dynamics across the model, in contrast to many existing studies that apply the fractional-order derivative only to the subpopulations on the left-hand side of the system. By extending the influence of α to the parameters on the right-hand side, the model achieves dimensional and temporal consistency, ensuring that all processes evolve under the same fractional framework. This is crucial for capturing the memory effects and hereditary dynamics inherent in biological systems, influencing not only the state variables but also recruitment, interactions, and decay rates. Scaling

Symbol	Description
$P_1(t)$	Population of susceptible bats at time t.
$P_2(t)$	Population of infectious bats at time t.
$P_3(t)$	Population of recovered bats at time t.
$Q(t)$	Level of environmental contamination at time t.
α	Order of the fractional derivative, capturing the memory effect in the dynamics.
${}_0^C\mathscr{D}_t^\alpha$	Caputo fractional derivative of order α.
β	Recruitment rate of susceptible bats into the population.
m	Natural mortality rate of bats.
λ_1	Transmission rate between susceptible and infectious bats.
λ_2	Transmission rate between susceptible bats and the contaminated environment.
r	Recovery rate of infectious bats.
δ	Rate at which infectious bats contribute to environmental contamination.
e	Rate of environmental decontamination.

TABLE 1. Description of the variables and parameters in the fractional-order system (1)

the recruitment rate and other parameters by α further reflects the non-instantaneous and temporally scaled nature of these processes, enhancing the realism of the model. By applying the same temporal scaling to parameters and subpopulations alike, this methodology provides a more holistic and robust representation of the underlying biological dynamics.

The first aim of this work is to examine the model's dynamics, and the second is to present an optimal contol environmental decontamination strategy. To this end, we structure this work in the following manner. In Section 2, we present some preliminary results that are fundamental to the development of the main analysis. This includes key definitions, lemmas, and propositions that will be used throughout the paper. In Section 3, the existence of solutions and equilibria is discussed. We establish the conditions under which the system has at least one solution. In Section 4, we perform a stability analysis of equilibria. The results are essential for understanding the long-term behavior of the system under different initial conditions. In Section 5,

we explore the fractional optimal control problem, including environmental decontamination as a control measure, aimed at minimizing the spread of the disease between bats. Section 6 provides numerical simulations to validate the theoretical findings, demonstrating the stability of the system under various values of the order derivative α. Moreover, we present a detailed numerical scheme that underpins the simulations of the states with and without the proposed control strategy. Finally, in Section 7, the paper concludes with a summary of the main findings, potential implications of the results, and suggestions for future research directions.

2. FOUNDATIONAL RESULTS

We begin by revisiting the definitions of the fractional-order integral, the Caputo fractional derivative, and the Mittag-Leffler function, as outlined in [19].

Definition 2.1. *The fractional integral of order $\alpha > 0$ of a function $f : R_+ \to R$ is defined as follows:*

$$I^{\alpha} f(t) = \frac{1}{\Gamma(\alpha)} \int_0^t (t-x)^{\alpha-1} f(x) \, dx,$$

where $\Gamma(.)$ is the Gamma function.

Definition 2.2. *The Caputo fractional derivative of order $\alpha > 0$ of a continuous function $f : R_+ \to R$ is given by:*

$$D^{\alpha} f(t) = I^{n-\alpha} D^n f(t),$$

where $D = \dfrac{d}{dt}$ and $n-1 < \alpha \leq n$, $n \in \mathbb{N}$. In particular, when $0 < \alpha \leq 1$, we have:

$$D^{\alpha} f(t) = \frac{1}{\Gamma(1-\alpha)} \int_0^t \frac{f'(x)}{(t-x)^{\alpha}} \, dx.$$

Definition 2.3. *Let $\alpha > 0$. The function E_{α} defined by*

$$E_{\alpha}(z) = \sum_{j=0}^{\infty} \frac{z^j}{\Gamma(\alpha j + 1)},$$

is called the Mittag-Leffler function of parameter α.

For biological reasons, we assume that the initial conditions of system (1) satisfy:

(2) $P_1(0) = \phi_1(0) \geq 0, \, P_2(0) = \phi_2(0) \geq 0, \, P_3(0) = \phi_3(0) \geq 0, \, Q(0) = \phi_4(0) \geq 0$

To establish the non-negativity of solutions with initial conditions (2), we also need the following lemmas.

Lemma 2.4. *([20]). Suppose that $g(t) \in C[a,b]$ and $D^{\alpha}g(t) \in C(a,b)$ for $0 < \alpha \leq 1$, then we have:*

$$g(t) = g(a) + \frac{1}{\Gamma(\alpha)}D^{\alpha}g(\xi)(t-a)^{\alpha} \quad a \leq \xi \leq t, \ \forall t \in (a,b].$$

Lemma 2.5. *([20]). Suppose that $g(t) \in C[a,b]$ and $D^{\alpha}g(t) \in C(a,b)$ for $0 < \alpha \leq 1$. If $D^{\alpha}g(t) \geq 0 \ \forall t \in (a,b]$, then $g(t)$ is non-decreasing for each $t \in [a,b]$. If $D^{\alpha}g(t) \leq 0 \ \forall t \in (a,b]$, then $g(t)$ is non-increasing for each $t \in [a,b]$.*

Theorem 2.6. *For any initial conditions satisfying (2), system (1) has a unique solution on $[0,+\infty)$. Moreover, this solution remains non-negative and bounded for all $t \geq 0$.*

Proof. In order to prove that the solution is bounded, we consider the following function:

$$T(t) = P_1(t) + P_2(t) + P_3(t) + Q(t).$$

Then we can obtain:

$$_{0}^{C}\mathscr{D}_t^{\alpha}T(t) \leq \beta^{\alpha} - \gamma T(t),$$

where $\gamma = \min\{m^{\alpha}, m^{\alpha} - \delta^{\alpha}, e^{\alpha}\}$. Hence,

$$T(t) \leq T(0)E_{\alpha}(-\gamma t^{\alpha}) + \frac{\beta^{\alpha}}{\gamma}[1 - E_{\alpha}(-\gamma t^{\alpha})],$$

where $E_{\alpha}(z) = \sum_{k=0}^{\infty}\frac{z^{\alpha}}{\Gamma(\alpha k+1)}$ is the Mittag-Leffler function of parameter α. Since $0 \leq E_{\alpha}(-\gamma t^{\alpha}) \leq 1$, we get:

$$T(t) \leq T(0) + \frac{\beta^{\alpha}}{\gamma},$$

which implies that P_1, P_2, P_3, and Q are bounded.

On the other hand, we have:

$$_{0}^{C}\mathscr{D}_t^{\alpha}P_1 \mid_{P_1=0} = \beta^{\alpha} > 0,$$

$$_{0}^{C}\mathscr{D}_t^{\alpha}P_2 \mid_{P_2=0} = \lambda_2^{\alpha}P_1Q \text{ for all } P_1, Q \geq 0,$$

$$_{0}^{C}\mathscr{D}_t^{\alpha}P_3 \mid_{P_3=0} = r^{\alpha}P_2 \text{ for all } P_2 \geq 0,$$

$$_{0}^{C}\mathscr{D}_t^{\alpha}Q \mid_{Q=0} = \delta^{\alpha}P_2 \text{ for all } P_2 \geq 0.$$

From Lemmas 2.4 and 2.5, it can be concluded that the solution of (1) remains non-negative.   ∎

3. EXISTENCE OF SOLUTION AND EQUILIBRIA

We will now establish the existence and uniqueness of the solution for the proposed model using the renowned fixed point theorem. Let $H(\mathscr{J})$ be a Banach space consisting of real-valued continuous functions defined on the interval $\mathscr{J} = [0,b]$, equipped with the sup norm. Define $\mathbb{G} = (H(\mathscr{J}))^4$ with the norm:

$$\|(P_1,P_2,P_3,Q)\| = \|P_1\| + \|P_2\| + \|P_3\| + \|Q\|,$$

where

$$\|P_1\| = \sup_{t \in \mathscr{J}} |P_1(t)|, \quad \|P_2\| = \sup_{t \in \mathscr{J}} |P_2(t)|, \quad \|P_3\| = \sup_{t \in \mathscr{J}} |P_3(t)|, \quad \|Q\| = \sup_{t \in \mathscr{J}} |Q(t)|.$$

The proposed model can then be expressed as:

(3)
$$
\begin{cases}
{}_0^C \mathscr{D}_t^\alpha P_1(t) = F_1(t,P_1), \\
{}_0^C \mathscr{D}_t^\alpha P_2(t) = F_2(t,P_2), \\
{}_0^C \mathscr{D}_t^\alpha P_3(t) = F_3(t,P_3), \\
{}_0^C \mathscr{D}_t^\alpha Q(t) = F_4(t,Q),
\end{cases}
$$

where

$$F_1(t,P_1) = \beta^\alpha - m^\alpha P_1 - \lambda_1^\alpha P_1 P_2 - \lambda_2^\alpha P_1 Q,$$

$$F_2(t,P_2) = \lambda_1^\alpha P_1 P_2 + \lambda_2^\alpha P_1 Q - (m^\alpha + r^\alpha) P_2,$$

$$F_3(t,P_3) = r^\alpha P_2 - m^\alpha P_3,$$

$$F_4(t,Q) = \delta^\alpha P_2 - e^\alpha Q.$$

Employing the Riemann-Liouville integral $\mathscr{I}_0^\alpha$ on both sides of system (3), we have:

$$P_1(t) - P_1(0) = \frac{1}{\Gamma(\alpha)} \int_0^t (t-x)^{\alpha-1} F_1(x,P_1) \, dx,$$

$$P_2(t) - P_2(0) = \frac{1}{\Gamma(\alpha)} \int_0^t (t-x)^{\alpha-1} F_2(x,P_2) \, dx,$$

$$P_3(t) - P_3(0) = \frac{1}{\Gamma(\alpha)} \int_0^t (t-x)^{\alpha-1} F_3(x, P_3) \, dx,$$

$$Q(t) - Q(0) = \frac{1}{\Gamma(\alpha)} \int_0^t (t-x)^{\alpha-1} F_4(x, Q) \, dx.$$

The functions F_1, F_2, F_3, and F_4 fulfill the Lipschitz condition whenever $P_1(t), P_2(t), P_3(t)$, and $Q(t)$ have an upper bound.

For any P_1, P_1^*, P_2 and P_2^*, we have:

$$\|F_1(t, P_1(t)) - F_1(t, P_1^*(t))\| \le \rho_1 \|P_1(t) - P_1^*(t)\|,$$

where $\rho_1 = m^\alpha + \lambda_1^\alpha \|P_2\| + \lambda_2^\alpha \|Q\|$. Following a similar approach, one obtains:

$$\|F_2(t, P_2(t)) - F_2(t, P_2^*(t))\| \le \rho_2 \|P_2(t) - P_2^*(t)\|,$$

$$\|F_3(t, P_3(t)) - F_3(t, P_3^*(t))\| \le \rho_3 \|P_3(t) - P_3^*(t)\|,$$

(4) $$\|F_4(t, Q(t)) - F_4(t, Q^*(t))\| \le \rho_4 \|Q(t) - Q^*(t)\|,$$

where

$$\rho_2 = \lambda_1^\alpha \|P_1\| + m^\alpha + r^\alpha,$$

$$\rho_3 = m^\alpha,$$

$$\rho_4 = e^\alpha.$$

This suggests that the Lipschitz condition is satisfied by all the functions. On the other hand, by using the recursive formula, we have:

$$P_{1,n}(t) - P_1(0) = \frac{1}{\Gamma(\alpha)} \int_0^t (t-x)^{\alpha-1} F_1(x, P_{1,n-1}) \, dx,$$

$$P_{2,n}(t) - P_2(0) = \frac{1}{\Gamma(\alpha)} \int_0^t (t-x)^{\alpha-1} F_2(x, P_{2,n-1}) \, dx,$$

$$P_{3,n}(t) - P_3(0) = \frac{1}{\Gamma(\alpha)} \int_0^t (t-x)^{\alpha-1} F_3(x, P_{3,n-1}) \, dx,$$

(5) $$Q_n(t) - Q(0) = \frac{1}{\Gamma(\alpha)} \int_0^t (t-x)^{\alpha-1} F_4(x, Q_{n-1}) \, dx,$$

By considering successive differences, the following results are obtained:

$$\Phi_{P_{1,n}}(t) = P_{1,n}(t) - P_{1,n-1}(t) = \frac{1}{\Gamma(\alpha)} \int_0^t (t-x)^{\alpha-1} (F_1(x, P_{1,n-1}) - F_1(x, P_{1,n-2})) \, dx,$$

$$\Phi_{P_{2,n}}(t) = P_{2,n}(t) - P_{2,n-1}(t) = \frac{1}{\Gamma(\alpha)} \int_0^t (t-x)^{\alpha-1} (F_2(x, P_{2,n-1}) - F_2(x, P_{2,n-2})) \, dx,$$

$$\Phi_{P_{3,n}}(t) = P_{3,n}(t) - P_{3,n-1}(t) = \frac{1}{\Gamma(\alpha)} \int_0^t (t-x)^{\alpha-1} (F_3(x, P_{3,n-1}) - F_3(x, P_{3,n-2})) \, dx,$$

$$\Phi_{Q_n}(t) = Q_n(t) - Q_{n-1}(t) = \frac{1}{\Gamma(\alpha)} \int_0^t (t-x)^{\alpha-1} (F_4(t, Q_{n-1}) - F_4(t, Q_{n-2})) \, dx.$$

Then

$$\left\| \Phi_{P_{1,n}}(t) \right\| \leq \frac{\rho_1}{\Gamma(\alpha)} \int_0^t (t-x)^{\alpha-1} \left\| \Phi_{P_{1,n-1}}(x) \right\| dx,$$

$$\left\| \Phi_{P_{2,n}}(t) \right\| \leq \frac{\rho_2}{\Gamma(\alpha)} \int_0^t (t-x)^{\alpha-1} \left\| \Phi_{P_{2,n-1}}(x) \right\| dx,$$

$$\left\| \Phi_{P_{3,n}}(t) \right\| \leq \frac{\rho_3}{\Gamma(\alpha)} \int_0^t (t-x)^{\alpha-1} \left\| \Phi_{P_{3,n-1}}(x) \right\| dx,$$

$$(6) \qquad \left\| \Phi_{Q_n}(t) \right\| \leq \frac{\rho_4}{\Gamma(\alpha)} \int_0^t (t-x)^{\alpha-1} \left\| \Phi_{Q_{n-1}}(x) \right\| dx.$$

Theorem 3.1. *A unique solution exists for the system (1) with any nonnegative initial condition for all $t \in [0, b]$ if the following condition holds:*

$$\rho_i \frac{b^\alpha}{\alpha \Gamma(\alpha)} < 1, \quad i = 1, 2, 3, 4.$$

Proof: As can be observed from (4), the functions F_1, F_2, F_3, and F_4 satisfy the Lipschitz condition. Thus,

$$\left\| \Phi_{P_{1,n}}(t) \right\| \leq \left(\rho_1 \frac{b^\alpha}{\alpha \Gamma(\alpha)} \right)^n \left\| P_1 - P_1(0) \right\|,$$

$$\left\| \Phi_{P_{2,n}}(t) \right\| \leq \left(\rho_2 \frac{b^\alpha}{\alpha \Gamma(\alpha)} \right)^n \left\| P_2 - P_2(0) \right\|,$$

$$\left\| \Phi_{P_{3,n}}(t) \right\| \leq \left(\rho_3 \frac{b^\alpha}{\alpha \Gamma(\alpha)} \right)^n \left\| P_3 - P_3(0) \right\|,$$

$$\left\| \Phi_{Q_n}(t) \right\| \leq \left(\frac{b^\alpha}{\alpha \Gamma(\alpha)} \right)^n \left\| Q - Q(0) \right\|.$$

Hence, the defined sequences exist and fulfill the conditions $\left\| \Phi_{P_{1,n}}(t) \right\| \to 0$, $\left\| \Phi_{P_{2,n}}(t) \right\| \to 0$, $\left\| \Phi_{P_{3,n}}(t) \right\| \to 0$, $\left\| \Phi_{Q_n}(t) \right\| \to 0$ as $n \to \infty$. Therefore, we deduce that the sequences $P_{1,n}$, $P_{2,n}$, $P_{3,n}$, and Q_n are Cauchy sequences within the Banach space $H(\mathscr{J})$ with the sup norm. Hence,

they are uniformly convergent [21]. By applying the limit theorem on all equations of (5), the limit of these sequences as $n \to \infty$ is the unique solution of the model. ∎

We now examine the existence of equilibrium points. The proposed model always possesses a Ebola-free equilibrium denoted $\mathscr{E}_0$ given as:

$$\mathscr{E}_0 \left(\frac{\beta^\alpha}{m^\alpha}, 0, 0, 0 \right).$$

The remaining equilibrium points of system (1) are determined by the following equations:

(7) $$F_1(t, P_1) = \beta^\alpha - m^\alpha P_1 - \lambda_1^\alpha P_1 P_2 - \lambda_2^\alpha P_1 Q = 0,$$

(8) $$F_2(t, P_2) = \lambda_1^\alpha P_1 P_2 + \lambda_2^\alpha P_1 Q - (m^\alpha + r^\alpha) P_2 = 0,$$

(9) $$F_3(t, P_3) = r^\alpha P_2 - m^\alpha P_3 = 0,$$

(10) $$F_4(t, Q) = \delta^\alpha P_2 - e^\alpha Q = 0.$$

From (7)-(10), we have:

$$P_2^* = \frac{\beta^\alpha - m^\alpha P_1^*}{m^\alpha + r^\alpha}, \quad P_3^* = \frac{r^\alpha}{m^\alpha} \frac{\beta^\alpha - m^\alpha P_1^*}{m^\alpha + r^\alpha}, \quad Q^* = \frac{\delta^\alpha}{e^\alpha} \frac{\beta^\alpha - m^\alpha P_1^*}{m^\alpha + r^\alpha}.$$

where $P_1^* = \frac{m^\alpha + r^\alpha}{\lambda_1^\alpha + \lambda_2^\alpha \frac{\delta^\alpha}{e^\alpha}}$. Since $P_2^* \geq 0$, we have $P_1^* \leq \frac{\beta^\alpha}{m^\alpha}$. We define the basic reproduction number $\mathscr{R}_0$ as follows:

$$\mathscr{R}_0 = \frac{\lambda_1^\alpha \beta^\alpha + \lambda_2^\alpha \frac{\delta^\alpha \beta^\alpha}{e^\alpha}}{m^\alpha (m^\alpha + r^\alpha)}.$$

Theorem 3.2. *Let $\mathscr{R}_0$ be defined as above.*

(i) When $\mathscr{R}_0 \leq 1$, system (1) has a single disease-free equilibrium given by $\mathscr{E}_0 \left(\frac{\beta^\alpha}{m^\alpha}, 0, 0, 0 \right)$.

(ii) If $\mathscr{R}_0 > 1$, the Ebola-free equilibrium persists, and system (1) also exhibits a unique endemic Ebola equilibrium of the form $\mathscr{E}^* \left(P_1^*, P_2^*, P_3^*, Q^* \right)$ with $P_1^* = \frac{m^\alpha + r^\alpha}{\lambda_1^\alpha + \lambda_2^\alpha \frac{\delta^\alpha}{e^\alpha}}$, $P_2^* = \frac{\beta^\alpha - m^\alpha P_1^*}{m^\alpha + r^\alpha}$, $P_3^* = \frac{r^\alpha}{m^\alpha} \frac{\beta^\alpha - m^\alpha P_1^*}{m^\alpha + r^\alpha}$, and $Q^* = \frac{\delta^\alpha}{e^\alpha} \frac{\beta^\alpha - m^\alpha P_1^*}{m^\alpha + r^\alpha}$.

4. ASYMPTOTIC STABILITY ANALYSIS

This section aims to analyze the stability of the equilibria.

Theorem 4.1. *The Ebola free equilibrium $\mathscr{E}_0$ is globally asymptotically stable when $\mathscr{R}_0 \leq 1$. However, it becomes unstable if $\mathscr{R}_0 > 1$.*

Proof. Consider the following Lyapunov functional

$$\mathscr{V}(t) = e^{\alpha} P_2 + \lambda_2^{\alpha} \frac{\beta^{\alpha}}{m^{\alpha}} Q.$$

The time derivative of $\mathscr{V}$ along the positive solution of (1) is expressed as

$$
\begin{aligned}
{}_0^C \mathscr{D}_t^{\alpha} \mathscr{V}(t) &= e_0^{\alpha C} P_2 + \lambda_2^{\alpha} \frac{\beta^{\alpha}}{m^{\alpha}} \mathscr{D}_t^{\alpha} Q, \\
&= \left(e^{\alpha} \lambda_1^{\alpha} P_1 - e^{\alpha}(m^{\alpha} + r^{\alpha}) + \delta^{\alpha} \lambda_2^{\alpha} \frac{\beta^{\alpha}}{m^{\alpha}} \right) P_2 + \lambda_2^{\alpha} e^{\alpha} \left(P_1 - \frac{\beta^{\alpha}}{m^{\alpha}} \right) Q, \\
&\leq \left(e^{\alpha} \lambda_1^{\alpha} \frac{\beta^{\alpha}}{m^{\alpha}} - e^{\alpha}(m^{\alpha} + r^{\alpha}) + \delta^{\alpha} \lambda_2^{\alpha} \frac{\beta^{\alpha}}{m^{\alpha}} \right) P_2 \\
&= e^{\alpha}(m^{\alpha} + r^{\alpha})(\mathscr{R}_0 - 1) P_2.
\end{aligned}
$$

As a result, ${}_0^C \mathscr{D}_t^{\alpha} \mathscr{V}(t) \leq 0$ for $\mathscr{R}_0 \leq 1$. Moreover, it is straightforward to verify that the largest compact invariant set within $\{(P_1, P_2, Q) \mid {}_0^C \mathscr{D}_t^{\alpha} \mathscr{V}(t) = 0\}$ is the singleton $\{\mathscr{E}_0\}$. Applying LaSalle's invariance principle [23], we conclude that $\mathscr{E}_0$ is globally asymptotically stable when $\mathscr{R}_0 \leq 1$. Through a simple computation, the characteristic equation at $\mathscr{E}_0$ is given by:

$$(m^{\alpha} + \lambda)^2 \left(\lambda^2 + \lambda \left(e^{\alpha} + m^{\alpha} + r^{\alpha} - \lambda_1^{\alpha} \frac{\beta^{\alpha}}{m^{\alpha}} \right) + e^{\alpha}(m^{\alpha} + r^{\alpha})(1 - \mathscr{R}_0) \right) = 0.$$

Let

$$\mathscr{H}(\lambda) = \left(\lambda^2 + \lambda \left(e^{\alpha} + m^{\alpha} + r^{\alpha} - \lambda_1^{\alpha} \frac{\beta^{\alpha}}{m^{\alpha}} \right) + e^{\alpha}(m^{\alpha} + r^{\alpha})(1 - \mathscr{R}_0) \right)$$

We observe that $\lim\limits_{\lambda \to +\infty} \mathscr{H}(\lambda) = +\infty$ and $\mathscr{H}(0) = e^{\alpha}(m^{\alpha} + r^{\alpha})(1 - \mathscr{R}_0)$. When $\mathscr{R}_0 > 1$, it follows that $\mathscr{H}(0) < 0$. Therefore, there exists a $\lambda_0 \in (0, +\infty)$ such that $\mathscr{H}(\lambda_0) = 0$, indicating that the characteristic equation at $\mathscr{E}_0$ has a positive root for $\mathscr{R}_0 > 1$. Consequently, $\mathscr{E}_0$ is unstable when $\mathscr{R}_0 > 1$. ■

Theorem 4.2. *When $\mathscr{R}_0 > 1$, the endemic Ebola equilibrium $\mathscr{E}^*$ is globally asymptotically stable.*

Proof. Define a Lyapunov functional as follows

$$
\begin{aligned}
\mathscr{K}(t) &= P_1(t) - P_1^* - P_1^* \ln\left(\frac{P_1(t)}{P_1^*} \right) + P_2(t) - P_2^* - P_2^* \ln\left(\frac{P_2(t)}{P_2^*} \right) \\
&\quad + \frac{g(S^*, P^*)}{\eta} \left(Q(t) - Q^* - Q^* \ln\left(\frac{Q(t)}{Q^*} \right) \right).
\end{aligned}
$$

$$\,_0^C\mathscr{D}_t^\alpha \mathscr{K}(t) = \left(1 - \frac{P_1^*}{P_1}\right)\,_0^C\mathscr{D}_t^\alpha P_1(t) + \left(1 - \frac{P_2^*}{P_2}\right)\,_0^C\mathscr{D}_t^\alpha P_2(t) + \frac{\lambda_2^\alpha P_1^*}{e^\alpha}\left(1 - \frac{Q^*}{Q}\right)\,_0^C\mathscr{D}_t^\alpha Q(t).$$

Using $\beta^\alpha = m^\alpha P_1^* + \lambda_1^\alpha P_1^* P_2^* + \lambda_2^\alpha P_1^* Q^* = m^\alpha P_1^* + (m^\alpha + r^\alpha)P_2^{**}$ et $\delta^\alpha P_2^* = e^\alpha Q^*$, we have

$$\begin{aligned}\,_0^C\mathscr{D}_t^\alpha \mathscr{K}(t) &= m^\alpha P_1^*\left(1 - \frac{P_1}{P_1^*}\right)\left(1 - \frac{P_1^*}{P_1}\right) + \lambda_1^\alpha P_1^* P_2^*\left(2 - \frac{P_1^*}{P_1} - \frac{P_1}{P_1^*}\right) \\ &\quad + \lambda_2^\alpha P_1^* Q^*\left(3 - \frac{P_1^*}{P_1} - \frac{P_1}{P_1^*}\frac{QP_2^*}{Q^*P_2} - \frac{Q^*P_2}{QP_2^*}\right).\end{aligned}$$

Given that the arithmetic mean is always greater than or equal to the geometric mean, it follows that

$$3 - \frac{P_1^*}{P_1} - \frac{P_1}{P_1^*}\frac{QP_2^*}{Q^*P_2} - \frac{Q^*P_2}{QP_2^*} \leq 0.$$

Thus, $\,_0^C\mathscr{D}_t^\alpha \mathscr{K}(t) \leq 0$ when $\mathscr{R}_0 > 1$. Moreover, the largest compact invariant set in $\{(P_1, P_2, Q) \mid \,_0^C\mathscr{D}_t^\alpha \mathscr{K}(t) = 0\}$ is the singleton $\{\mathscr{E}^*\}$. Thanks to LaSalle's invariance principle, $\mathscr{E}^*$ is globally asymptotically stable for $\mathscr{R}_0 > 1$. ∎

5. FRACTIONAL OPTIMAL CONTROL PROBLEM

In bats, Ebola virus can be shed through saliva, feces, or urine, contaminating the environment. In this section, we propose to control the spread of Ebola between bats by the strategy of decontamination of environment. The main aim is to minimize the number of infectious bats while reducing the cost associated with this strategy.

5.1. Environmental Decontamination as Control Measure.

By reducing viral persistence in roosting or feeding areas, decontamination decreases the likelihood of bats becoming infected through environmental contact. This is achieved by introducing environmental decontamination as a preventive measure with a time-dependent control $c(t)$. Therefore, we formulate the following fractional optimal control problem:

(11)
$$\min J(P_2(t), c(t)) = \int_0^{t_f} \left[P_2(t) + A\sigma c^2(t)\right] dt$$

subject to the fractional control system:

$$
(12) \quad
\begin{cases}
D^\alpha P_1(t) = \beta^\alpha - m^\alpha P_1 - \lambda_1^\alpha P_1 P_2 - (1 - c(t))\lambda_2^\alpha P_1 Q, \\[2mm]
D^\alpha P_2(t) = \lambda_1^\alpha P_1 P_2 - (m^\alpha + r^\alpha) P_2 + (1 - c(t))\lambda_2^\alpha P_1 Q, \\[2mm]
D^\alpha P_3(t) = r^\alpha P_2 - m^\alpha P_3, \\[2mm]
D^\alpha Q(t) = \delta^\alpha P_2 - e^\alpha Q.
\end{cases}
$$

with initial conditions:

$$
(13) \qquad P_1(0) = P_0^1 \geq 0, \quad P_2(0) = P_0^2 \geq 0, \quad P_3(0) = P_0^3 \geq 0, \quad Q(0) = Q_0 \geq 0.
$$

The parameter A is a positive weight, adjusting the overall cost to a suitable scale, σ is a parameter related to the extent of the decontamination effort, and $A\sigma c^2(t)$ is the cost of applying control effort c. t_f is the duration of the control program. The set of admissible control functions is:

$$
(14) \qquad \mathscr{U} = \left\{ c(t) \in L^\infty(0, t_f) : 0 \leq c(t) \leq c_{\max} \leq 1, \forall t \in [0, t_f] \right\}.
$$

To establish the existence of the optimal control for our problem, we ensure the following conditions: First, the set of admissible controls $\mathscr{U}$ is non-empty, convex, and closed in $L^\infty(0, t_f)$. Second, for any control $c(t) \in \mathscr{U}$, the fractional state equations have unique solutions, ensuring the well-posedness of the state system. Third, the cost functional J is bounded from below, which prevents the cost from becoming unbounded and ensures feasibility. Finally, the cost functional J is lower semi-continuous, which is essential for applying the direct method in the calculus of variations to conclude the existence of an optimal control. By satisfying these conditions, we can confirm the existence of an optimal control for the given fractional control system.

5.2. Optimality conditions. To derive the necessary optimality conditions for our fractional optimal control problem, we define the Hamiltonian function as:

$$
\begin{aligned}
\mathscr{H} = {} & P_2(t) + A\sigma c^2(t) + \xi_1(t) \left(\beta^\alpha - m^\alpha P_1 - \lambda_1^\alpha P_1 P_2 - (1 - c(t))\lambda_2^\alpha P_1 Q \right) \\[2mm]
& + \xi_2(t) \left(\lambda_1^\alpha P_1 P_2 - (m^\alpha + r^\alpha) P_2 + (1 - c(t))\lambda_2^\alpha P_1 Q \right) \\[2mm]
(15) \qquad & + \xi_3(t) \left(r^\alpha P_2 - m^\alpha P_3 \right) + \xi_Q(t) \left(\delta^\alpha P_2 - e^\alpha Q \right),
\end{aligned}
$$

where $\xi_1(t)$, $\xi_2(t)$, $\xi_3(t)$, and $\xi_Q(t)$ are the adjoint variables corresponding to $P_1(t)$, $P_2(t)$, $P_3(t)$, and $Q(t)$, respectively.

Applying Theorem 4.1 and Lemma 4.2 from [24], the necessary conditions for the optimality of (11) are:

$$\,_0^C D_t^\alpha P_1(t) = \beta^\alpha - m^\alpha P_1(t) - \lambda_1^\alpha P_1(t)P_2(t) - (1 - c(t))\lambda_2^\alpha P_1(t)Q(t),$$

$$\,_0^C D_t^\alpha P_2(t) = \lambda_1^\alpha P_1(t)P_2(t) + (1 - c(t))\lambda_2^\alpha P_1(t)Q(t) - (m^\alpha + r^\alpha)P_2(t),$$

$$\,_0^C D_t^\alpha P_3(t) = r^\alpha P_2(t) - m^\alpha P_3(t),$$

(16) $$\,_0^C D_t^\alpha Q(t) = \delta^\alpha P_2(t) - e^\alpha Q(t),$$

and

$$\,_0^C D_t^\alpha \xi_1(t') = -\xi_1(t') \left(m^\alpha + \lambda_1^\alpha P_2(t') + (1 - c(t'))\lambda_2^\alpha Q(t') \right),$$

$$\,_0^C D_t^\alpha \xi_2(t') = -1 + \lambda_1^\alpha P_1(t')(\xi_2(t') - \xi_1(t')) + r^\alpha \xi_3(t') + \delta^\alpha \xi_Q(t')$$

$$+ \left((1 - c(t'))\lambda_2^\alpha P_1(t') - (m^\alpha + r^\alpha) \right) \xi_2(t'),$$

$$\,_0^C D_t^\alpha \xi_3(t') = -m^\alpha \xi_3(t'),$$

(17) $$\,_0^C D_t^\alpha \xi_Q(t') = -e^\alpha \xi_Q(t').$$

with $t' = t_f - t$, positive initial data and transversality conditions:

(18) $$\xi_1(t_f) = \xi_2(t_f) = \xi_3(t_f) = \xi_Q(t_f) = 0.$$

Taking the partial derivative of $\mathscr{H}$ with respect to c:

$$\frac{\partial \mathscr{H}}{\partial c} = 2A\sigma c(t) + \xi_1(t)\lambda_2^\alpha P_1 Q - \xi_2(t)\lambda_2^\alpha P_1 Q$$

Setting this equal to zero for optimality:

$$2A\sigma c(t) = (\xi_2(t) - \xi_1(t))\lambda_2^\alpha P_1 Q$$

So, the optimal control is given by:

$$c^*(t) = \min \left(c_{\max}, \max \left(0, \frac{(\xi_2(t) - \xi_1(t))\lambda_2^\alpha P_1 Q}{2A\sigma} \right) \right)$$

6. NUMERICAL SIMULATIONS

In this section, we will conduct numerical simulations to achieve two primary objectives, first, to validate the theoretical stability results, and second, to illustrate the effectiveness of the optimal control strategy in reducing the number of infectious bats. These simulations will also showcase the model's dynamics for variant orders of the derivative α. The initial conditions are:

$$P_1(0) = 400, \quad P_2(0) = 10, \quad P_2(0) = 100, \quad Q(0) = 4,$$

6.1. Stability. We simulate system (1) using the following parameter values: $\beta^\alpha = 1.5$, $m^\alpha = 0.0003$, $\lambda_1^\alpha = 4.5 \times 10^{-6}$, $\lambda_2^\alpha = 1.3 \times 10^{-4}$, $r^\alpha = 0.1$, $\delta^\alpha = 0.02$, and $e^\alpha = 0.8$. A simple calculation yields $\mathscr{R}_0 = 0.9383$. Consequently, system (1) has a single Ebola-free equilibrium, $\mathscr{E}_0(5000, 0, 0, 0)$, which is globally asymptotically stable. This result is illustrated in Figure 1, where we observe that the disease eventually dies out.

Next, we simulate the scenario where the basic reproduction number exceeds one. For this, we set $\lambda_1^\alpha = 2.5 \times 10^{-5}$ while keeping the other parameter values unchanged. This results in $\mathscr{R}_0 = 3.4201 > 1$. As a result, system (1) has a unique endemic Ebola equilibrium $\mathscr{E}^*(1759.8457, 23.5361, 0.5887)$, which is globally asymptotically stable. This implies that the Ebola virus persists within the bat population, making the disease endemic. This outcome is shown in figure 2.

The contour plot in figure 3 illustrates the relationship between the basic reproduction number $\mathscr{R}_0$, which serves as the threshold determining the stability behavior of the system, and the fractional infection rates λ_1^α and λ_2^α for Ebola in the bat population, considering the parameters: $\beta^\alpha = 1.5$, $m^\alpha = 0.0003$, $r^\alpha = 0.041$, $\delta^\alpha = 0.02$, and $e^\alpha = 0.8$. The horizontal axis represents λ_1^α, while the vertical axis represents λ_2^α, with contour lines showing constant levels of $\mathscr{R}_0$.

At low values of both λ_1^α and λ_2^α, $\mathscr{R}_0$ is minimal, indicating effective control of disease spread. As either λ_1^α or λ_2^α increases, $\mathscr{R}_0$ grows significantly, reflecting the additive contribution of the two infection pathways to disease transmission. Even if one of the rates remains low, a high value in the other is sufficient to maintain a high $\mathscr{R}_0$, emphasizing the importance of controlling both pathways.

The contour corresponding to $\mathscr{R}_0 = 1$ marks the critical threshold between controlled conditions ($\mathscr{R}_0 < 1$) and outbreak scenarios ($\mathscr{R}_0 > 1$). Keeping λ_1^α and λ_2^α in the region where $\mathscr{R}_0 < 1$ is essential to prevent the spread of Ebola among bats. However, controlling the transmission rate from infectious bats to susceptible individuals (λ_1^α) is challenging due to the high mobility and interactions within bat populations. This suggests prioritizing the control of transmission from the contaminated environment (λ_2^α), which may involve targeted environmental decontamination or habitat management to reduce the risk of indirect transmission.

Overall, the contour plot emphasizes the need for targeted interventions to reduce both λ_1^α and λ_2^α, as high infection rates in either pathway can sustain the outbreak. Achieving and maintaining $\mathscr{R}_0 < 1$ is critical for effective control of Ebola in the bat population.
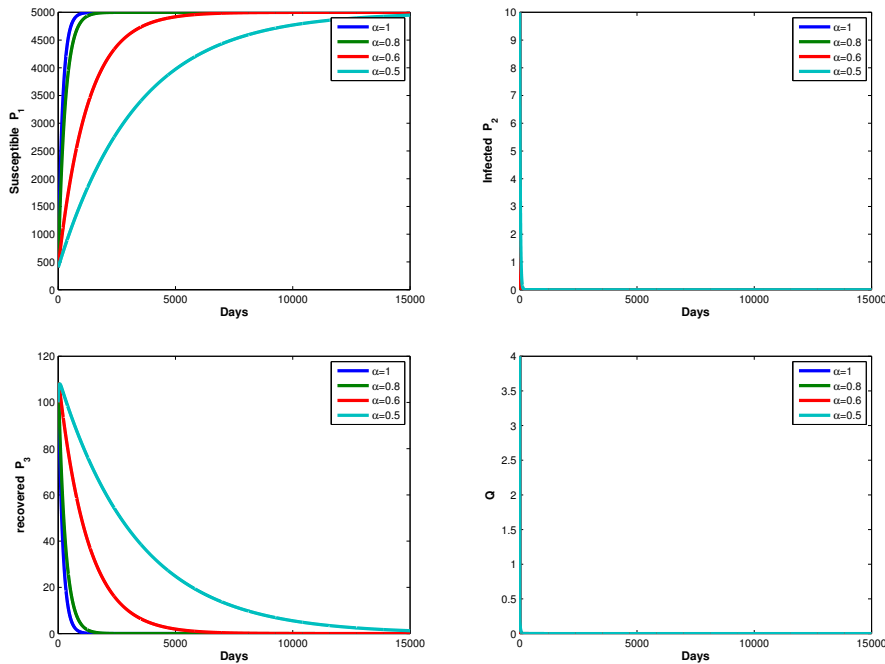

FIGURE 1. Stability of the Ebola free equilibrium $\mathscr{E}_0$.

6.2. Control measure. The numerical scheme implemented in the MATLAB code utilizes an iterative forward-backward sweep method to solve the optimal control problem with fractional-order dynamics. The method begins by integrating the state equations forward in time using a fractional Euler-type method, capturing the system's memory effects. Subsequently, the adjoint variables, are integrated backward in time. The control variable is iteratively updated based
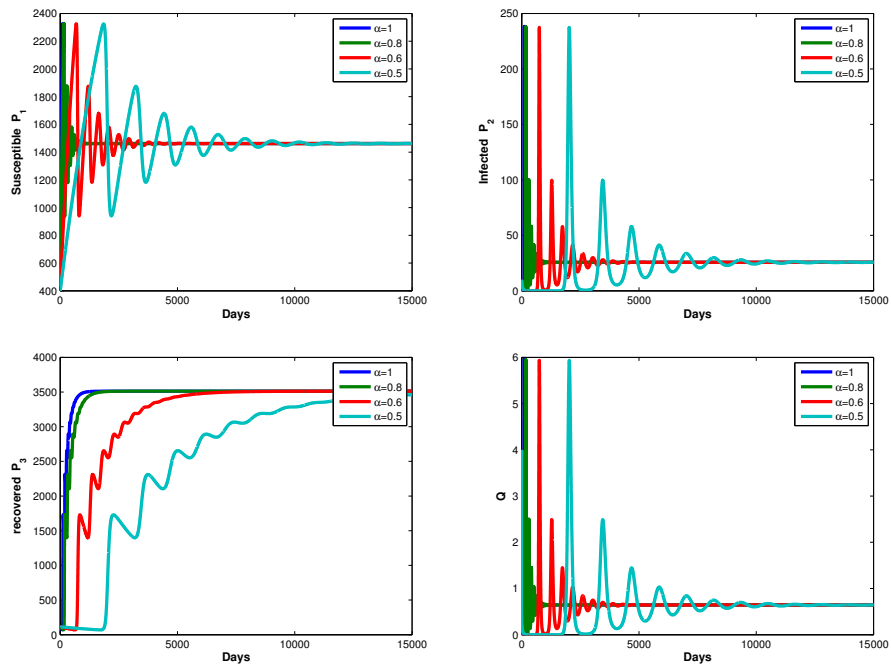
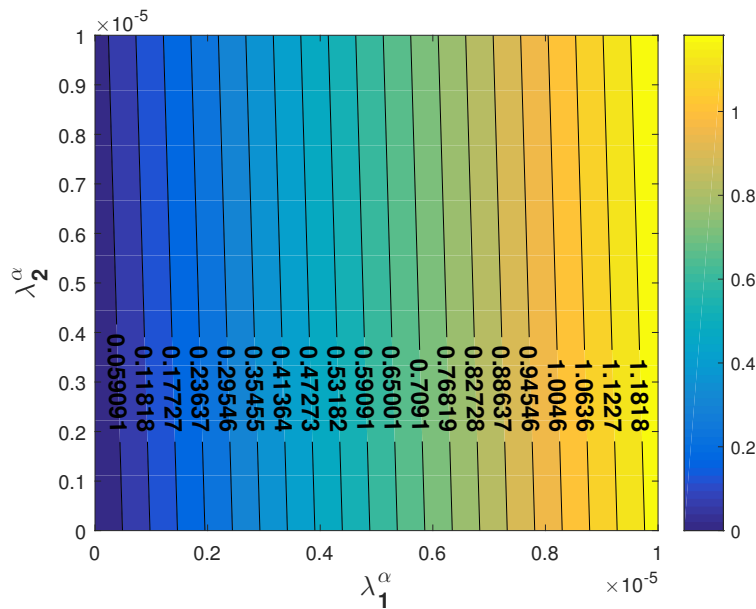FIGURE 2. Stability of the endemic Ebola equilibrium $\mathscr{E}^*$.

FIGURE 3. Contour Plot of the basic reproduction number with respect to the fractional infection rates λ_1^α and λ_2^α for $\beta^\alpha = 1.5$, $m^\alpha = 0.0003$, $r^\alpha = 0.041$, $\delta^\alpha = 0.02$ and $e^\alpha = 0.8$

on the adjoint variables, ensuring the optimality of the solution. The process repeats until convergence is achieved, providing a robust solution that balances control effectiveness with system dynamics. Without restricting generality, we consider the case where $\alpha = 0.8$. The numerical sheme is described as follows.

Step 1: Initialization

Set the initial conditions:

$$P_1(0) = 400, \quad P_2(0) = 10, \quad P_3(0) = 100, \quad Q(0) = 4$$

Set the adjoint variables at the final time:

$$\xi_1(t_{\text{final}}) = 0, \quad \xi_2(t_{\text{final}}) = 0, \quad \xi_3(t_{\text{final}}) = 0, \quad \xi_Q(t_{\text{final}}) = 0$$

Set the control variable:

$$c(0) = 0$$

Parameters:

$$\beta^\alpha = 1.5, \quad m^\alpha = 0.0003, \quad \lambda_1^\alpha = 2.5 \times 10^{-5}, \quad \lambda_2^\alpha = 1.3 \times 10^{-4}$$

$$r^\alpha = 0.041, \quad \delta^\alpha = 0.02, \quad e^\alpha = 0.8, \quad A = 1, \quad \sigma = 0.01, \quad c_{\max} = 1, \quad \alpha = 0.8$$

Time discretization:

$$t_0 = 0, \quad t_{\text{final}} = 1000, \quad \Delta t = 0.01, \quad n = \text{ceil}\left(\frac{t_{\text{final}}}{\Delta t}\right) = 100000$$

Step 2: Forward Sweep for State Variables with Control

For $i = 0$ to $n - 1$, do:

$$P_1(i+1) = P_1(i) + \frac{(\Delta t)^\alpha}{\Gamma(\alpha+1)}[\beta^\alpha - m^\alpha P_1(i) - \lambda_1^\alpha P_1(i)P_2(i) - (1-c(i))\lambda_2^\alpha P_1(i)Q(i)]$$

$$P_2(i+1) = P_2(i) + \frac{(\Delta t)^\alpha}{\Gamma(\alpha+1)}[\lambda_1^\alpha P_1(i)P_2(i) + (1-c(i))\lambda_2^\alpha P_1(i)Q(i) - (m^\alpha + r^\alpha)P_2(i)]$$

$$P_3(i+1) = P_3(i) + \frac{(\Delta t)^\alpha}{\Gamma(\alpha+1)}[r^\alpha P_2(i) - m^\alpha P_3(i)]$$

$$Q(i+1) = Q(i) + \frac{(\Delta t)^\alpha}{\Gamma(\alpha+1)}[\delta^\alpha P_2(i) - e^\alpha Q(i)]$$

Step 3: Backward Sweep for Adjoint Variables

For $i = n - 1$ down to 0, do:

$$\xi_1(i) = \xi_1(i+1) - \frac{(\Delta t)^\alpha}{\Gamma(\alpha+1)} \left[-\xi_1(i+1)(m^\alpha + \lambda_1^\alpha P_2(i+1) + (1 - c(i+1))\lambda_2^\alpha Q(i+1)) \right]$$

$$\xi_2(i) = \xi_2(i+1) - \frac{(\Delta t)^\alpha}{\Gamma(\alpha+1)} \left[-1 + \lambda_1^\alpha P_1(i+1)(\xi_2(i+1) - \xi_1(i+1)) + r^\alpha \xi_3(i+1) + \delta^\alpha \xi_Q(i+1) \right.$$

$$\left. + (1 - c(i+1))\lambda_2^\alpha P_1(i+1)\xi_2(i+1) - (m^\alpha + r^\alpha)\xi_2(i+1) \right]$$

$$\xi_3(i) = \xi_3(i+1) - \frac{(\Delta t)^\alpha}{\Gamma(\alpha+1)} \left[-m^\alpha \xi_3(i+1) \right]$$

$$\xi_Q(i) = \xi_Q(i+1) - \frac{(\Delta t)^\alpha}{\Gamma(\alpha+1)} \left[-e^\alpha \xi_Q(i+1) \right]$$

Step 4: Update Control Variable

Compute the new control:

$$c_{\text{new}}(i) = \min\left(c_{\max}, \max\left(0, \frac{(\xi_2(i) - \xi_1(i))\lambda_2^\alpha P_1(i)Q(i)}{2A\sigma} \right) \right)$$

Step 5: Check for Convergence

If:

$$\|\mathbf{c}_{\text{new}} - \mathbf{c}\| < \text{tolerance}$$

then break the loop.

Update control:

$$\mathbf{c} = \mathbf{c}_{\text{new}}$$

Step 6: Forward Sweep for State Variables without Control

For $i = 0$ to $n - 1$, do:

$$P_1(i+1) = P_1(i) + \frac{(\Delta t)^\alpha}{\Gamma(\alpha+1)} \left[\beta^\alpha - m^\alpha P_1(i) - \lambda_1^\alpha P_1(i)P_2(i) - \lambda_2^\alpha P_1(i)Q(i) \right]$$

$$P_2(i+1) = P_2(i) + \frac{(\Delta t)^\alpha}{\Gamma(\alpha+1)} \left[\lambda_1^\alpha P_1(i)P_2(i) + \lambda_2^\alpha P_1(i)Q(i) - (m^\alpha + r^\alpha)P_2(i) \right]$$

$$P_3(i+1) = P_3(i) + \frac{(\Delta t)^\alpha}{\Gamma(\alpha+1)} \left[r^\alpha P_2(i) - m^\alpha P_3(i) \right]$$

$$Q(i+1) = Q(i) + \frac{(\Delta t)^\alpha}{\Gamma(\alpha+1)} \left[\delta^\alpha P_2(i) - e^\alpha Q(i) \right]$$
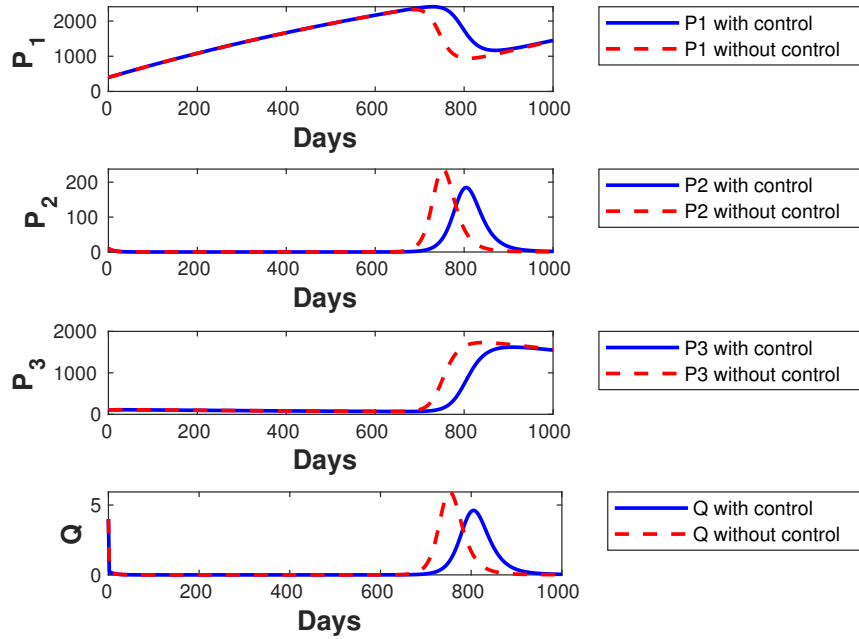
FIGURE 4. classes with and without environmental decontamination control
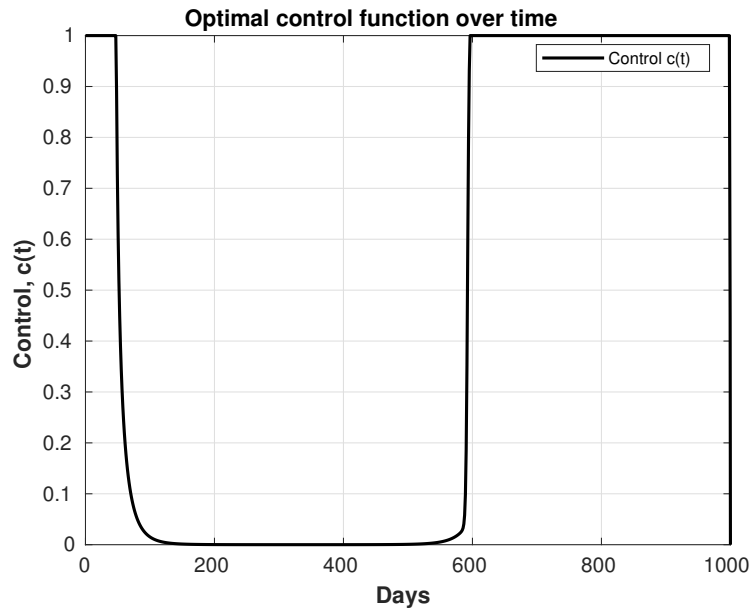

FIGURE 5. optimal control function with respect to time

Figure 4 displays the results comparing the dynamics of the four variables (P_1, P_2, P_3, and Q) over time (measured in days) under two different scenarios: with control (blue solid lines)

and without control (red dashed lines). The top plot illustrates the behavior of susceptible bats P_1, where it is observed that without control, P_1 gradually increases and levels off after approximately 800 days. In contrast, with control, P_1 follows a similar initial trend but then decreases sharply around 800 days, suggesting that the control effectively reduces P_1 at a crucial point in time.

The second plot shows the dynamics of infectious bats P_2, that is being minimized, where a significant peak is observed without control around 800 days. With control, the peak is moderated, indicating that the control is successfully managing the growth of P_2 and possibly preventing a large spike. The third plot depicts the recovered bats P_3 dynamics, where the variable increases in both scenarios but reaches a higher value without control. The control scenario results in slower growth and stabilization at a lower value, reflecting the effectiveness of the control in limiting P_3's rise.

Finally, the bottom plot shows Q's behavior, where a noticeable peak occurs around 800 days without control. With control, the peak is lower and more delayed, indicating the control's success in mitigating rapid increases in Q. Overall, across all plots, the control strategy demonstrates significant impact by reducing peaks, stabilizing the system, and preventing sharp increases, thereby effectively managing the dynamics of the variables P_1, P_2, P_3, and Q over time.

On the other hand, The figure 5 illustrates the optimal control function $c(t)$ over time, representing the control measure of environmental decontamination. The function $c(t)$ starts at its maximum value, indicating full activation of decontamination efforts from the beginning, and gradually decreases to nearly zero around 250 days, suggesting a reduction in efforts as the environment becomes cleaner. Between 250 and 600 days, $c(t)$ remains close to zero, indicating minimal or no decontamination activity during this period. However, around 600 days, $c(t)$ rises sharply back to its maximum value, reflecting a reactivation of decontamination efforts due to renewed contamination. The control measure then decreases again towards the end of the period, signaling a return to a cleaner state with reduced decontamination needed. Overall, $c(t)$ exhibits an adaptive strategy, increasing during periods of high contamination and decreasing when the environment stabilizes.

7. Conclusion

The relationship between bats and the Ebola virus highlights the intricate interplay between wildlife and human health. As natural reservoirs, bats play a vital role in maintaining the virus in the environment, with human exposure often occurring through direct or indirect contact. Mathematical models are crucial for understanding the dynamics of disease transmission and evaluating potential control strategies. These frameworks provide a systematic approach to simulate complex interactions between bats, the virus, and their shared environment. In this study, we aim to capture the extended influence of bat behavior and environmental factors on the persistence of the virus through a robust modeling approach. These models offer a more accurate representation of the interactions between Ebola virus reservoirs and their environment.

Through comprehensive stability analysis, this study highlights the critical role of the basic reproduction number (R_0) in determining the persistence or eradication of Ebola within bat populations. For $R_0 \leq 1$, the Ebola-free equilibrium is globally stable, indicating that the disease will eventually disappear. Conversely, when $R_0 > 1$, the endemic equilibrium becomes stable, signifying the sustained presence of the virus within the population. These findings provide valuable insights into the long-term dynamics of Ebola outbreaks, offering a theoretical basis for understanding and managing the disease under various ecological and epidemiological conditions.

An additional key contribution of this study is the integration of an optimal control strategy focused on environmental decontamination. This approach effectively mitigates the spread of Ebola virus disease (EVD) by targeting environmental reservoirs, reducing infection rates within bat populations, and lowering spillover risks to other species, including humans. Numerical simulations validate the theoretical results, demonstrating that environmental decontamination significantly reduces the number of infectious bats and minimizes environmental contamination. These findings underscore the practical importance of implementing targeted disease control strategies to manage zoonotic diseases like Ebola.

Future research can expand on this framework by exploring alternative control strategies, such as habitat modifications or enhanced environmental management practices. Additionally,

incorporating stochasticity or spatial heterogeneity could better simulate real-world complexities. Future studies could also focus on modeling spillover dynamics between bats and other species, including humans, to provide a deeper understanding of zoonotic transmission pathways and identify critical intervention points. This study provides a robust foundation for advancing infectious disease modeling and guiding public health efforts to mitigate the risks of spillover events.

CONFLICT OF INTERESTS

The authors declare that there is no conflict of interests.

REFERENCES

[1] WHO, Ebola: West Africa, March 2014-2016. https://www.who.int/emergencies/situations/ebola-outbreak-2014-2016-West-Africa.

[2] WHO, Ebola: North Kivu/Ituri, Democratic Republic of the Congo, August 2018-June 2020. https://www.who.int/emergencies/situations/Ebola-2019-drc-.

[3] E.M. Leroy, B. Kumulungui, X. Pourrut, et al. Fruit Bats as Reservoirs of Ebola Virus, Nature 438 (2005), 575–576. https://doi.org/10.1038/438575a.

[4] T.J. Lunn, R.T. Jackson, P.W. Webala, et al. Kenyan Free-Tailed Bats Demonstrate Seasonal Birth Pulse Asynchrony with Implications for Virus Maintenance, EcoHealth 21 (2024), 94–111. https://doi.org/10.1007/s10393-024-01674-x.

[5] M. Ermonval, S. Morand, Viral Zoonoses: Interactions and Factors Driving Virus Transmission, Viruses 16 (2023), 9. https://doi.org/10.3390/v16010009.

[6] E. Metta, H. Mohamed, P. Kusena, et al. Community Perspectives of Ebola Viral Disease in High-Risk Transmission Border Regions of Tanzania: A Qualitative Inquiry, BMC Public Health 24 (2024), 2766. https://doi.org/10.1186/s12889-024-20305-2.

[7] M. Leach, Preventing and Preparing for Pandemics, in: Regenerative Farming and Sustainable Diets, Routledge, London, 2024: pp. 36–42. https://doi.org/10.4324/9781032684369-7.

[8] E.M. Leroy, A. Epelboin, V. Mondonge, et al. Human Ebola Outbreak Resulting from Direct Exposure to Fruit Bats in Luebo, Democratic Republic of Congo, 2007, Vector-Borne Zoonotic Dis. 9 (2009), 723–728. https://doi.org/10.1089/vbz.2008.0167.

[9] A.M. Saéz, S. Weiss, K. Nowak, et al. Investigating the Zoonotic Origin of the West African Ebola Epidemic, EMBO Mol. Med. 7 (2015), 17–23. https://doi.org/10.15252/emmm.201404792.

[10] G. Fiorillo, P. Bocchini, J. Buceta, A Predictive Spatial Distribution Framework for Filovirus-Infected Bats, Sci. Rep. 8 (2018), 7970. https://doi.org/10.1038/s41598-018-26074-4.

[11] B. Tsanou, J.M.S. Lubuma, A.J.O. Tassé, H.M. Tenkam, Dynamics of Host-Reservoir Transmission of Ebola with Spillover Potential to Humans, Electron. J. Qual. Theory Differ. Equ. 2018 (2018), 14. https://doi.org/10.14232/ejqtde.2018.1.14.

[12] Z. El Rhoubari, H. Besbassi, K. Hattaf, N. Yousfi, Mathematical Modeling of Ebola Virus Disease in Bat Population, Discret. Dyn. Nat. Soc. 2018 (2018), 5104524. https://doi.org/10.1155/2018/5104524.

[13] M.A. Almuqrin, P. Goswami, S. Sharma, et al. Fractional Model of Ebola Virus in Population of Bats in Frame of Atangana-Baleanu Fractional Derivative, Results Phys. 26 (2021), 104295. https://doi.org/10.1016/j.rinp.2021.104295.

[14] Z. El Rhoubari, K. Hattaf, T. Regragui, Mathematical Analysis of a Generalized Reaction-Diffusion Model of Ebola Transmission in Bats, Commun. Math. Biol. Neurosci. 2024 (2024), 83. https://doi.org/10.28919/cmbn/8727.

[15] G. Ossa, S. Kramer-Schadt, A.J. Peel, A.K. Scharf, C.C. Voigt, The Movement Ecology of the Straw-Colored Fruit Bat, Eidolon Helvum, in Sub-Saharan Africa Assessed by Stable Isotope Ratios, PLoS ONE 7 (2012), e45729. https://doi.org/10.1371/journal.pone.0045729.

[16] J. Fahr, M. Abedi-Lartey, T. Esch, M. Machwitz, R. Suu-Ire, M. Wikelski, D.K.N. Dechmann, Pronounced Seasonal Changes in the Movement Ecology of a Highly Gregarious Central-Place Forager, the African Straw-Coloured Fruit Bat (Eidolon Helvum), PLOS ONE 10 (2015), e0138985. https://doi.org/10.1371/journal.pone.0138985.

[17] A.J. Peel, D.R. Sargan, K.S. Baker, et al. Continent-Wide Panmixia of an African Fruit Bat Facilitates Transmission of Potentially Zoonotic Viruses, Nat. Commun. 4 (2013), 2770. https://doi.org/10.1038/ncomms3770.

[18] R.D. Abdul-Wahhab, M.M. Eisa, S.L. Khalaf, The Study of Stability Analysis of the Ebola Virus via Fractional Model, Partial Differ. Equ. Appl. Math. 11 (2024), 100792. https://doi.org/10.1016/j.padiff.2024.100792.

[19] I. Podlubny, Fractional Differential Equations: An Introduction to Fractional Derivatives, Fractional Differential Equations, to Methods of Their Solution and Some of Their Applications, Academic Press, San Diego, 1998.

[20] Z.M. Odibat, N.T. Shawagfeh, Generalized Taylor's Formula, Appl. Math. Comput. 186 (2007), 286–293. https://doi.org/10.1016/j.amc.2006.07.102.

[21] A. Taylor, D. Lay, Introduction to Functional Analysis, Wiley, New York, 1980.

[22] I.S. Gradshteyn, I.M. Ryzhik, Routh-Hurwitz Theorem, in Tables of Integrals, Series, and Products, Academic Press, 2000.

[23] J.P. LaSalle, The Stability of Dynamical Systems, SIAM, Philadelphia, PA, 1976.

[24] H. Kheiri, M. Jafari, Optimal Control of a Fractional-Order Model for the HIV/AIDS Epidemic, Int. J. Biomath. 11 (2018), 1850086. https://doi.org/10.1142/S1793524518500869.